Microfabrication by electrochemical metal removal

by M. Datta

Recent advances in the development of electrochemical metal-removal processes for microfabrication are reviewed in this paper. After a brief description of the process, several important parameters are identified that determine the material-removal rate, shape control, surface finishing, and uniformity. The influence of surface film properties, mass transport, and current distribution on microfabrication performance are discussed. Several examples of microelectronic component fabrication are presented. These examples demonstrate the challenges and opportunities offered by electrochemical metal removal in microfabrication.

Introduction

Material-removal techniques are among the key processing technologies that are used in the fabrication of microelectronic components [1]. These methods are popularly known as etching techniques. Dry vacuum processes for thin-film etching are based on plasma-assisted processes and include ion etching, plasma etching, and reactive ion etching [1]. Ion etching is a physical process, whereas plasma etching involves a chemical reaction. Reactive ion etching is a combination of both physical and chemical effects contributing to material removal. In ion etching, ions are extracted from a gaseous plasma and accelerated to the substrate, where the surface is eroded by momentum transfer. Plasma etching employs a glow discharge to generate active species such as atoms or free radicals. The active species diffuse to the substrate,

where they react with the surface to produce volatile products. Addition of reactive gases to the ion source (reactive ion etching) enhances the physical etch rate and introduces chemical etching as well. These processes are particularly employed in the semiconductor industry for ultralarge-scale integration (ULSI) because of their ability to remove material with precision. However, some of the disadvantages that are inherent in dry-etching techniques include high equipment cost, lack of selectivity, and problems arising from redeposition on the sample and deposition on the vacuum chamber. Dry-etching techniques are used for precision etching of thin films involving very small amounts of material removal. Lately, concern has intensified about the safety, environmental impact, and disposal of the toxic gases used in plasmaassisted dry etching.

Wet chemical etching involves removal of unwanted material by the exposure of the workpiece to an etchant. The exposed material is oxidized by the reactivity of the etchant to yield reaction products that are transported from the surface by the medium. Chemical etching converts a solid insoluble material to a soluble form by dissolving the extended lattice of metal atoms so that these atoms can enter the solution as soluble compounds. This is accompanied by removal of electrons from the metal (oxidation). These electrons are accepted by the etchant, which acts as an oxidizing agent in chemical etching. The metal-removal reaction typically involves several sequential steps, the dissolution kinetics being controlled either by the chemical reactivity of the species involved (activation-controlled) or by the speed at which the reaction product is removed from the surface and the fresh reactant is supplied to the surface (diffusion- or

*Copyright 1998 by International Business Machines Corporation. Copying in printed form for private use is permitted without payment of royalty provided that (1) each reproduction is done without alteration and (2) the *Journal* reference and IBM copyright notice are included on the first page. The title and abstract, but no other portions, of this paper may be copied or distributed royalty free without further permission by computer-based and other information-service systems. Permission to *republish* any other portion of this paper must be obtained from the Editor.

0018-8646/98/\$5.00 © 1998 IBM



Through-slots micromachined in a 50- μ m-thick stainless steel sheet using a 5-M sodium nitrate electrolyte jet. The nozzle diameter is 200 μ m [7].

mass-transport-controlled). Temperature variations also profoundly influence the kinetics of metal-removal reaction.

Wet chemical etching baths contain chemicals that are generally aggressive and toxic [2], thus posing safety and disposal problems. In many wet-etching manufacturing processes, waste treatment and disposal costs often surpass actual etching processing costs. The everincreasing cost of incineration and the imposition of landfilling restrictions are the main reasons behind the need for developing alternative processes.

Electrochemical metal removal is an alternative wetetching process where the workpiece is made an anode in an electrolytic cell in which a salt solution is used as an electrolyte and controlled metal removal takes place by application of an external current. Several nonconventional machining processes such as electrochemical machining (ECM) and electropolishing are based on the principle of electrochemical metal removal [3, 4]. The ECM process has been used predominantly in the production of turbine engine parts and for other aerospace applications, but applications of ECM also exist in the production of automotive components, medical implants, appliance parts, artillery projectiles, gun-barrel rifling, etc. because of its ability to machine complex features and complicated contours without machining marks, burrs, or surface stresses. ECM is used to perform machining operations analogous to broaching, turning, and die sinking, while static machining with a stationary tool is used to deburr, polish, and/or radius components. The rapid metalremoval rate along with the advantage of nonconsumed tooling makes it an attractive process for metal shaping and finishing. However, electrochemical metal removal has received little attention so far in the microelectronics industry. Recent investigations of the development of advanced electrochemical metal-removal processes demonstrate that the ECM concepts can be effectively

used in the removal and patterning of conducting films that are of interest in the electronics industry [5, 6].

Electrochemical micromachining (EMM)

Application of ECM in the processing of thin films and in the fabrication of microstructures is referred to as electrochemical micromachining (EMM). Compared to predominantly used chemical etching, the EMM process offers better control and flexibility, requires very little monitoring and control, and has minimum safety and environmental concerns [5, 6]. A variety of metals and alloys can be machined by EMM. EMM is now receiving considerable attention in the electronics and other high-technology industries, particularly as an alternate, "greener" method of processing metallic parts [5, 6].

Most of the thin films of metals and alloys, including conducting ceramics and highly corrosion-resistant alloys, that are of interest in the microelectronics industry can be anodically dissolved in neutral salt electrolytes such as sodium nitrate, sulfate, or chloride. In these electrolytes, the dissolved metal ions form hydroxide precipitates which remain in suspended form in solution and can be easily filtered, thus significantly minimizing problems of safety and waste disposal. Hydrogen evolution is generally the main cathodic reaction. The cathode, therefore, remains unaltered. Accumulation of reaction products in solution and depletion of bath components are of little concern in EMM, thus making it a simpler and more environmentally friendly manufacturing process.

Microfabrication by EMM may involve maskless or through-mask material removal. Thin-film patterning by maskless EMM requires highly localized material removal induced by the impingement of a fine electrolytic jet [5, 7]. Investigation of jet and laser-jet EMM demonstrated that neutral salt solutions can be effectively used for high-speed micromachining of many metals and alloys. An example of such an investigation is shown in Figure 1, which demonstrates the feasibility of employing an electrolytic jet for generating complicated patterns in metallic foils and substrates. Other examples of maskless EMM include microfinishing of components and removal of unwanted layers of thin films by electromilling [8].

EMM in conjunction with a photoresist mask is of considerable interest in microelectronic fabrication. Through-mask EMM involves selective metal dissolution from unprotected areas of a one- or two-sided photoresist-patterned workpiece. Through-mask metal removal by wet etching is accompanied by undercutting of the photoresist and is generally isotropic in nature. In isotropic etching, the material is removed both vertically and laterally at the same rate. This is particularly the case in chemical etching, where the etch boundary usually recedes at a 45° angle relative to the surface [2]. In EMM, however, the metal-removal rate in the lateral direction may be

significantly reduced through proper consideration of mass transport and current distribution [5]. Etch factor is defined as the ratio of the amount of straight-through etch to the amount of undercut [6]. For applications requiring high aspect ratio, minimized undercutting of the photoresist and a high value of etch factor are desirable.

EMM performance criteria

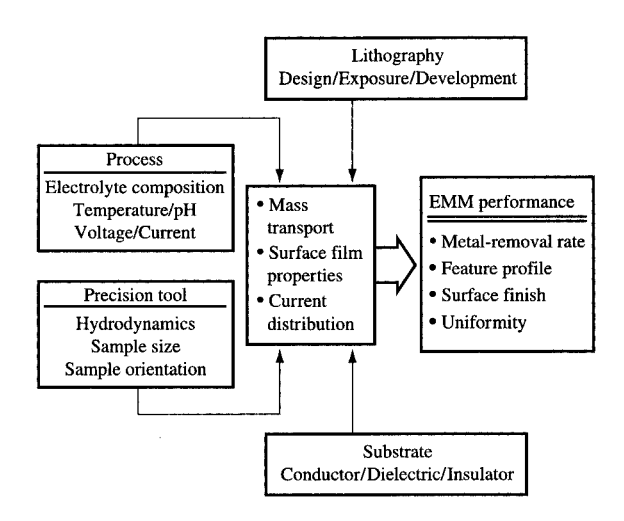
The metal-removal rate, microfeature profile, surface finish, and uniformity of metal removal are some of the performance criteria that determine the technical feasibility of a metal-removal process. In EMM, these criteria are dependent on the ability of the system to provide desired mass-transport rates, current distribution, and surface film properties at the active surface (Figure 2). An understanding of the metal-electrolyte interaction under high-rate anodic dissolution conditions is a prerequisite for optimizing process parameters such as electrolyte composition and voltage/current. The development of precision tools requires an understanding of the influence of hydrodynamics, current distribution, and process parameters on the EMM performance. A precision tool should provide conditions of desired current distribution and a high rate of uniform mass transport at the dissolving surface [5].

In through-mask processes, additional issues related to lithography processing are critical to achieving desired performance. Production of the master artwork, surface preparation, choice of proper photoresist, and imaging are extremely important in the successful implementation of an etching process. Since parts produced by this process are a direct reflection of the master artwork, it is essential that all aspects of preparing the artwork are understood. These include a priori knowledge of the metal-removal rate and etch factor. Imaging is another important step, the objective of which is to reproduce the artwork features as closely as possible onto the workpiece. The imaging process capability is measured by its resolution. In EMM, careful design of the walls and height of the photoresist provide opportunities to alter current distribution that reduce the photoresist undercutting. The conductivity of the substrate material is also important in influencing the current distribution of a dissolving thin film.

The material-removal rate in EMM depends on the specific electrochemical behavior of the metal/electrolyte system and is determined by the applied current density according to the Faraday law [9]. The material-removal rate r, in cm/s, is given by

$$r = \frac{IM}{nFA\rho},\tag{1}$$

where I is the current in amperes, M is the molecular weight of the dissolved material in g/mole, n is the



Relationship between EMM performance and processing/tooling parameters.

apparent dissolution valence, F is the Faraday constant, A is the surface area in cm², and ρ is density in g/cm³. The value of n can be determined from weight-loss measurements using Equation (2),

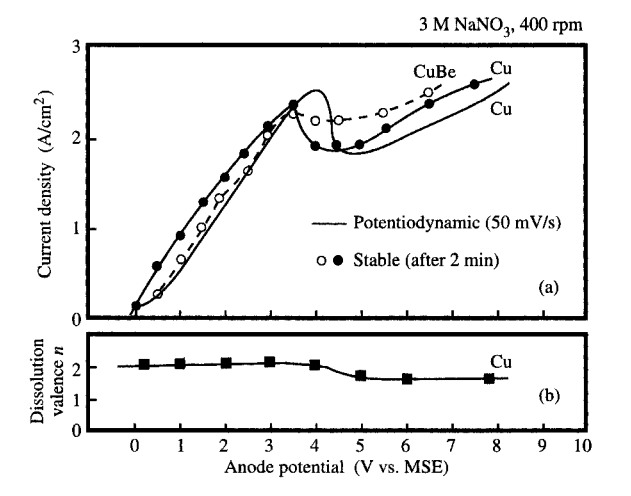
$$n = \frac{ItM}{\Delta WF},\tag{2}$$

where t is the dissolution time in seconds and ΔW is the anodic weight loss in grams.

With proper considerations of high electrolyte-flow velocities and high current efficiency for metal dissolution, extremely high metal-removal rates can be obtained. A knowledge of the dependence of n on the applied voltage/current density is essential in order to determine the operating conditions such that slight variations in voltage/current are not associated with changes in the dissolution valence. The literature data on experimentally determined dissolution valence for different metal-electrolyte systems under active and transpassive conditions are summarized in Reference [9].

Mass-transport effects

Mass transport processes have profound influence on the EMM performance. These processes determine the maximum rate of an electrodissolution reaction, thus giving rise to a so-called *limiting current*; mass-transport-controlled anodic reactions affect the morphology of dissolved surfaces; and finally, mass-transport processes influence the macroscopic and microscopic current



Anodic polarization behavior of Cu and CuBe (a) and dissolution valence as a function of anode potential for Cu (b) (see Footnote 2). Experiments were performed with rotating-disk electrodes (RDEs) at 400 rpm in a 3-M sodium nitrate electrolyte. The anode potential is reported vs. a mercury sulfate electrode (MSE).

distribution on the workpiece. An understanding of masstransport effects is, therefore, a prerequisite for the development of EMM processes. In the following, a simple description of mass transport in an anodic dissolution process is described.

In an EMM process, an increase in current density leads to an increase in the rate of metal ion production at the anode. When the metal ion concentration at the surface exceeds the saturation limit, precipitation of a thin salt film occurs. The anodic polarization curve under these conditions exhibits a limiting current plateau. The limiting current increases with increasing electrolyte flow in a channel cell or with increasing rotation speed in an RDE system. The limiting current density is, therefore, controlled by convective mass transport [5].

For an anodic reaction that is controlled by convective mass transport, the anodic limiting current density, $i_{\scriptscriptstyle \ell}$, is given by

$$i_{\ell} = nFD \frac{C_{\text{sat}}}{\delta}, \tag{3}$$

where D is the effective diffusion coefficient that takes into account the contributions from transport by migration [10, 11], $C_{\rm sat}$ is the surface concentration, and δ is the diffusion-layer thickness.

The Nernst diffusion-layer concept has frequently been used to obtain a simplified description of mass-transport effects in high-rate anodic dissolution of metals. A

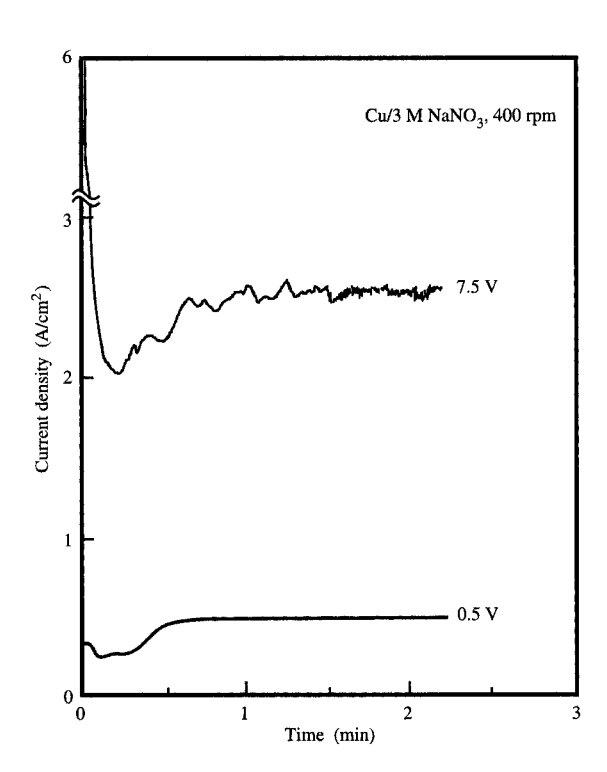
stagnant diffusion layer of thickness δ is thus assumed to exist at the anode. Inside the diffusion layer, a concentration gradient exists, and the transport occurs exclusively by diffusion. Outside the diffusion layer, transport occurs by convection, and the electrolyte concentration is assumed to be constant. The thickness of the anodic diffusion layer depends on hydrodynamic conditions and is given by

$$\delta = \frac{L}{Sh},\tag{4}$$

where L is a characteristic length and Sh is the Sherwood number that represents the nondimensional mass-transport rate. The Sherwood number can also be regarded as the normalized or nondimensionalized diffusion layer thickness. An exhaustive list of derived expressions describing $Sh = f(Re, Sc)^{\top}$ are available in the literature for various flow situations and geometries [12].

The process of EMM involves dissolution from a cavity formed by localized dissolution. The effect of fluid flow on

¹ Re represents the Reynolds number, and Sc the Schmidt number.



Potentiostatic current transients for Cu rotating-disk electrodes in a 3-M sodium nitrate electrolyte at 0.5 and 7.5 V (see Footnote 2). The electrode rotation speed is 400 rpm.

the convective mass transport in a cavity is expressed by the Peclet number, Pe, which is defined as follows:

$$Pe = \frac{vL}{D},\tag{5}$$

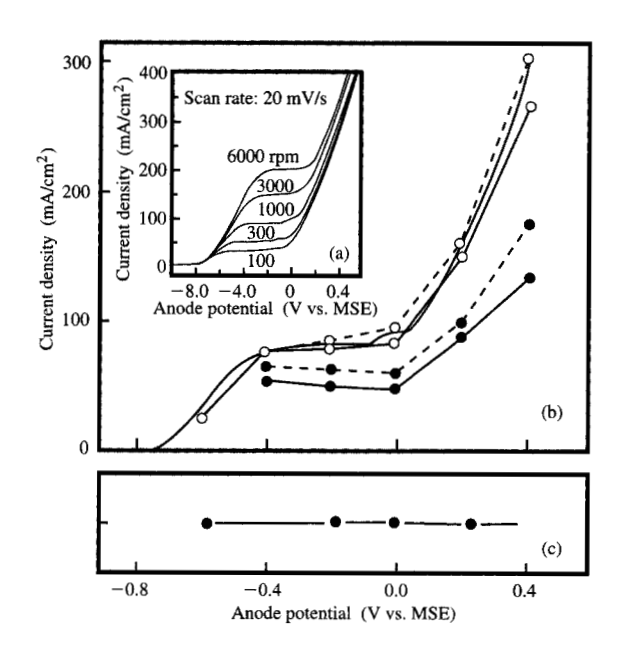
where v is the flow velocity and the characteristic length L is the width of the cavity. The influence of the Peclet number on the average mass-transfer rate in a cavity has been correlated on the basis of experimentally measured average mass-transfer coefficients during etching of patterned Cu samples [13]. The following empirical correlation was obtained:

$$Sh_{av} = 0.3(L/H)^{0.83}Pe^{0.33},$$
 (6)

where *H* is the cavity depth. Equation (6) has been found to be in agreement with the average mass-transfer rates calculated by solving the equations for Stokes flow by the finite-element method and by a combination of the boundary integral method and Lighthill boundary-layer analysis [13].

Surface films and their role

Anodic dissolution of copper and molybdenum in sodium nitrate electrolyte is taken as two different systems to demonstrate the importance of surface films in EMM.² The experimental data were obtained with rotating-disk electrodes using potentiodynamic and potentiostatic techniques. Anodic weight-loss experiments were performed to determine the dissolution valence using Faraday's law [Equation (1)]. Figure 3 shows the anodic polarization curves for Cu and an alloy of Cu containing 2% Be. The steady-state potentiostatic data were obtained from current transients at different potentials given in Figure 4. Qualitatively similar anodic polarization behavior is obtained by both potentiostatic and potentiodynamic techniques. At potentials up to about 3.5 V (vs. mercury sulfate electrode, MSE), active dissolution of copper leads to a sharp increase in current with increasing potential. Beyond this potential, a current plateau is observed. At high potentials, the current once again increases, rather slowly, with increasing anode potential leading to transpassive dissolution [9]. Note that except for a slightly better-defined limiting current, the anodic polarization behavior is not changed by the presence of a small amount of Be in copper. At low potentials, where current increases sharply with increasing potential, the current transients show a slow increase in current before reaching a steady value. At high potentials, the anodic current shoots to very high values, then drops sharply, indicating the formation of salt films at the surface. The current transients eventually reach a steady-state value. In the transpassive potential region, metal dissolution takes place through a

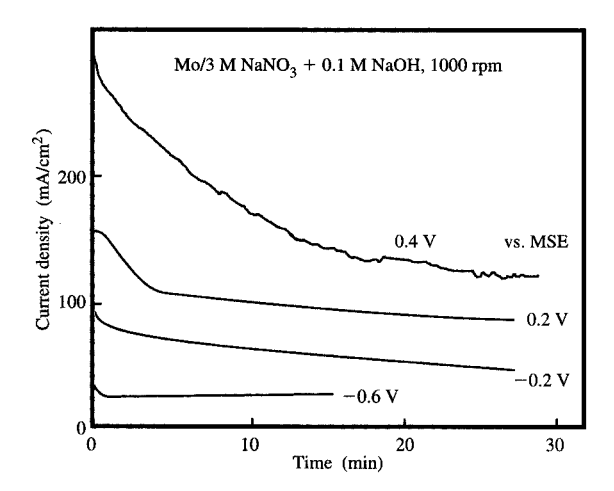


Anodic polarization behavior of molybdenum (a), (b) and its dissolution valence as a function of anode potential (c) in an electrolyte containing a mixture of 3 M sodium nitrate and 0.1 M sodium hydroxide (see Footnote 2). The anode potential is reported vs. a mercury sulfate electrode (MSE). Experiments were performed with rotating-disk electrodes. Part (a) shows potentio-dynamic polarization curves at different rotation speeds of the anode using a potential scan of 20 mV/s. Part (b) shows time-dependent potentiostatic polarization curves at a constant rotation speed of 1000 rpm: initial current, o--o; after 1 min, o—o; after 10 min, •-•; after 20 min, •-•; and potentiodynamic polarization curve at a scan rate of 20 mV/s, —. Part (c) shows dissolution valence data obtained from potentiostatic weight-loss measurements at a constant rotation speed of 1000 rpm.

stable salt film at the surface. The presence of such films on the dissolving surface is a key to obtaining microsmooth surface and uniformity of feature profile in microfabrication. Also included in Figure 3 are the dissolution valence data obtained from anodic weight-loss measurements. In the active region, a constant dissolution valence of 2 is obtained. The value slowly drops with increasing potential, reaching a constant value of 1.5 in the transpassive potential region. Under these conditions, copper dissolution leads to simultaneous production of cuprous and cupric ions [14].

Anodic polarization of molybdenum in a sodium nitrate electrolyte at neutral pH led to a linear increase in anodic current with increasing potential, the current–potential curves being independent of electrode rotation speed. In an alkaline solution, on the other hand, the

² M. Datta and W. J. Yu, unpublished work.



Potentiostatic current transients for molybdenum rotating-disk electrodes in a mixture of 3 M sodium nitrate and 0.1 M sodium hydroxide solution at different anode potentials (see Footnote 2). The electrode rotation speed is 1000 rpm.

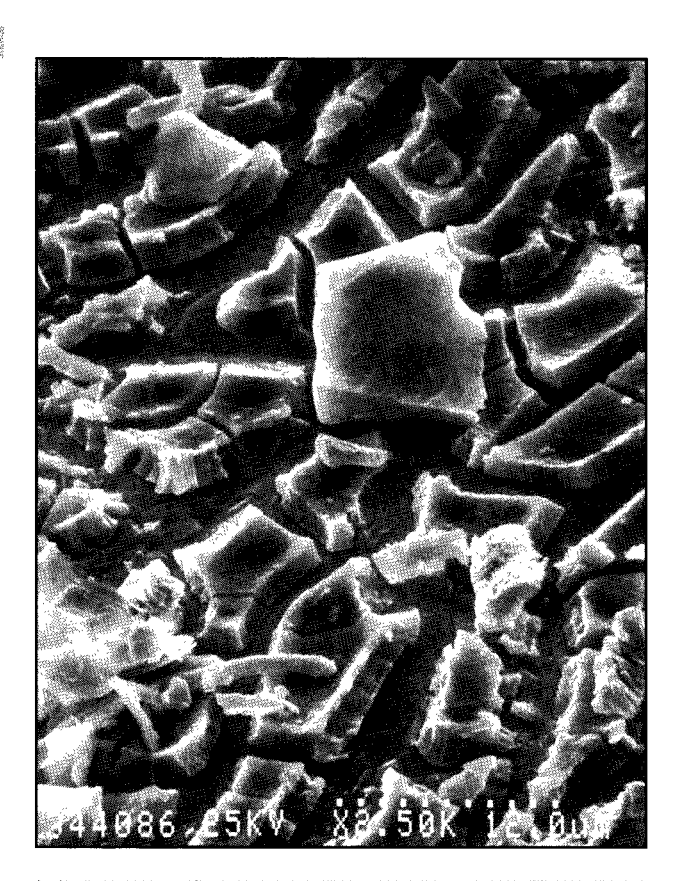
current-potential curve exhibited a mass-transportcontrolled limiting current, as shown in Figure 5(a). The time-dependent polarization curves shown in Figure 5(b) were derived from potentiostatic current transients, which showed a gradual decrease in current, particularly at high potentials (Figure 6). It is interesting to note that the dissolution stoichiometry during anodic dissolution of molybdenum remained constant in its hexavalent state independent of anode potential [Figure 5(c)]. All of the above data indicate that anodic dissolution of molybdenum takes place in the presence of surface films that grow in thickness. A scanning-electron-microscopic (SEM) photograph of a molybdenum surface dissolved in an alkaline sodium nitrate solution in the transpassive potential region is shown in Figure 7. Thick surface films were observed which adhered to the surface during molybdenum dissolution. These surface films flaked out on drying and required impinging water jets for their removal. The anode surfaces underneath were electropolished. Formation of such thick films on the dissolving surface induces nonuniformities during microfabrication by EMM. A detailed investigation has been undertaken to minimize the film growth on molybdenum while maintaining a stable salt film at the surface [15].

The formation of salt films on the anode influences the surface morphology and the rate of dissolution during ECM and electropolishing [9, 10, 15, 16]. Different studies have conclusively demonstrated that two distinctly

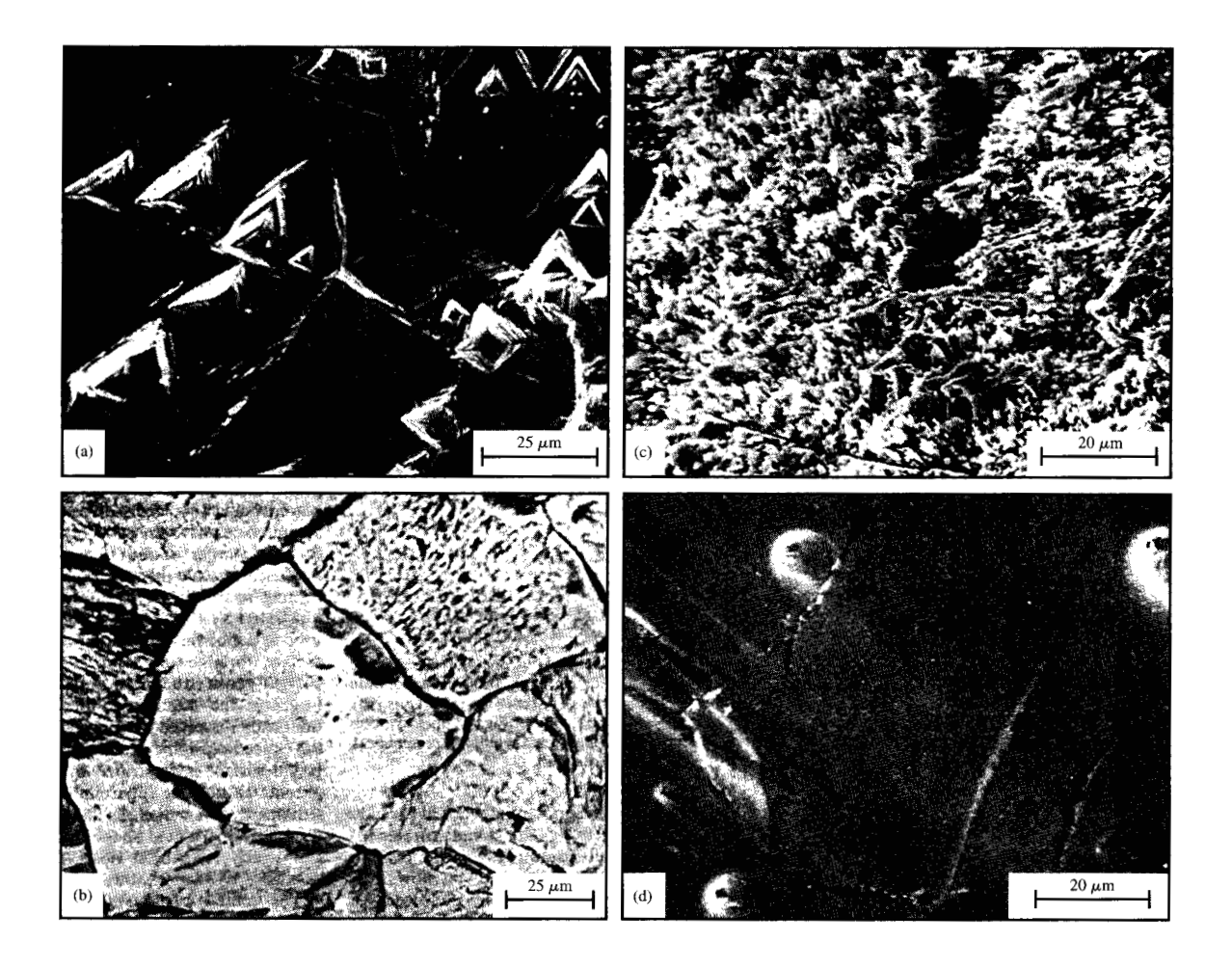
different surface morphologies result from dissolution (Figure 8). At current densities lower than the limiting current density, surface etching is observed which, depending on the metal—electrolyte combination, reveals crystallographic steps and etch pits, preferred grain-boundary attack, or finely dispersed microstructure. Anodic dissolution under these conditions leads to extremely rough surfaces. On the other hand, formation of salt films at limiting or higher current densities suppresses the influence of crystallographic orientation and surface defects on the dissolution process, leading to microfinishing. The presence of salt films has also been found to have a significant effect on the current distribution during EMM of photoresist-masked anodes [11, 15, 17, 18].

Current distribution and shape evolution modeling

Application of through-mask EMM in microfabrication requires an understanding of some of the complexities and challenges associated with the process. The most



SEM photograph of a molybdenum anode after dissolution at $0.0~\rm V$ vs. MSE, corresponding to the limiting current plateau of Figure 5 (see Footnote 2).

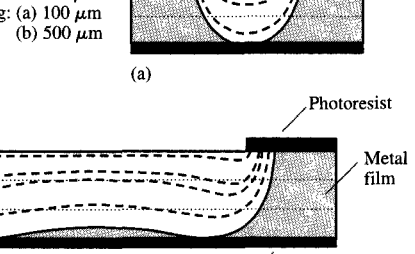


SEM photograph of surfaces after dissolution below the limiting current (a), (b), (c) and above the limiting current (d). Experiments were performed in a flow channel cell at an electrolyte flow velocity of 1000 cm/s [10, 16]. Part (a), nickel dissolved in 5 M NaCl at 5 A/cm²; Part (b), iron dissolved in 5 M NaCl at 5 A/cm²; Part (c), nickel dissolved in 5 M NaNO₃ at 25 A/cm²; Part (d), nickel dissolved in 5 M NaNO₃ at 25 A/cm².

important of these is the elimination of loss of electrical contact in the case of one-sided EMM. Other challenges include the ability of EMM to provide uniformity of metal removal on the sample scale and on the feature scale, straight and smooth walls, and minimized undercutting for fine features. These factors are governed primarily by current distribution and mass-transport conditions on the dissolving sample.

Some of the issues mentioned above have recently been investigated in our laboratory [19–21]. Experimental results and mathematical modeling of shape evolution during different stages of EMM have provided some insight into the problems of island formation and loss of electrical contact described above. The influence on shape

evolution of the photoresist thickness, initial opening, and the thickness of metal film undergoing EMM has been determined by numerical calculation of current distribution on the cavity features. The shape evolution depends on photoresist thickness, feature opening, and the metal-film thickness [19–21]. At the initial stage of EMM, the current is concentrated more at the edges than in the middle. As EMM proceeds, the current concentration shifts gradually from the edges to the middle of the feature. The latter condition is desirable, since this ensures complete removal of the material from the center. For a given photoresist and metal-film thickness, the shift in the current concentration is dependent on the initial feature dimension that is exposed to the current, as shown



Insulato

(b)

Mathematically modeled shapes of evolving features during different stages of EMM for different photoresist openings (a), (b). Island of unetched material in the middle of a large opening (b) is caused by current maximum at the edges of the dissolving surface. From [6], reproduced with permission.

in Figure 9. For small openings [Figure 9(a)], the current concentration moves to the center of the feature before the metal film is etched. For large openings [Figure 9(b)], the metal film may not be thick enough for the current concentration to shift to the middle. Under these conditions, because of the faster rate of dissolution at the edges, an island of material remains unetched, losing electrical contact with the rest of the metallic surface and thus bringing the EMM process to an end. The problem of island formation can, in principle, be resolved by converting the situation of Figure 9(b) into a number of narrow openings, as in Figure 9(a). This can be achieved by introducing dummy photoresist artwork [19]. It is essential, however, that the dimensions of the dummy photoresist artwork match the undercutting of the photoresist from both sides, so that upon completion of EMM the dummy photoresist is removed, yielding a clean, straight-walled micromachined trench.

Designing the dimensions of the dummy artwork requires a knowledge of undercutting and its dependence on the photoresist opening dimensions, which can be experimentally determined [19]. For a 75- μ m-thick stainless steel film sample, an average value of undercutting was found to be 50 μ m, independent of opening dimensions. On the basis of the experimental results, photoresist artwork design modifications were made to include dummy artwork that converted openings larger than 700 μ m into a set of smaller openings using 100- μ m-wide photoresist lines as dividers. EMM of samples with dummy artwork demonstrated that the

problems related to the loss of electrical contact can indeed be eliminated by reducing the size of the opening [19].

The above concept of introducing dummy photoresist artwork requires a delicate balance between lateral dissolution and vertical dissolution on one hand and the width of the dummy photoresist on the other. It has been demonstrated that the choice of proper dummy dimensions can lead to the elimination of island formation during microfabrication of components on flat samples. However, for samples involving topographic features, the last traces of unetched materials may be difficult to remove by EMM. In such cases, EMM may be followed by a brief application of another etching technique to effectively remove the unetched islands without significantly altering the wall angle.

In a recent study we have also investigated the influence of the photoresist wall angle on shape evolution during through-mask EMM [20]. At the beginning of the EMM process, the primary current distribution at the anode surface is very sensitive to the photoresist wall angle. However, as the EMM process continues, the evolving cavity causes significant redistribution of the current along the electrode surface, the current distribution becoming more uniform. Acute-angled masks improve the directionality of through-mask EMM by reducing the undercut for thin metal films [20]. However, the influence of the mask wall angle diminishes with increasing metal-film thickness [20].

Experimental EMM tools

Development of an effective EMM process requires careful design and fabrication of a tool that provides desired current-distribution and mass-transport conditions at the dissolving surface. The electrolyte delivery system is one of the main considerations in the design of a precision tool. Different electrolyte delivery systems that are applicable in EMM include channel flow, electrolytic jet, slotted jet, and multinozzle systems [16, 22–24]. Sample orientation, electrical contact, and provisions for filtration are some of the other important design aspects that must be taken into account.

Figure 10 shows a one-sided EMM tool.³ The tool consists of a driving mechanism (XYZ table) for sample movement, an electrolyte delivery system in the form of a multinozzle assembly, an electrolyte reservoir, and electrolyte pumping and filtration units. The multinozzle assembly also acts as the cathode. The sample is held in a sample holder, which is attached to the XYZ table and is moved at a constant speed over the multinozzle cathode. The interelectrode spacing is kept constant between 1 and 3 mm. A 1-in.-wide multinozzle-flow assembly provides high-speed electrolyte impingement at the dissolving

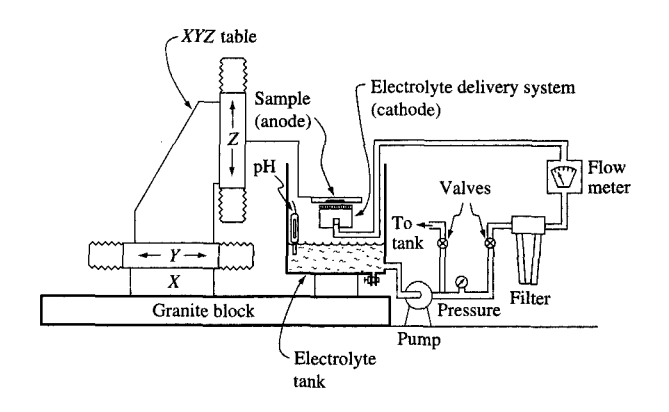
³ M. Datta, unpublished work.

surface, thus permitting effective removal of the dissolved products and of the heat generated by joule heating. The tool can be used for EMM of samples of different sizes. The active area at a given time during micromachining is defined by the electrolyte in contact with the sample. Within the interelectrode gap, the electrolyte emanating from the multinozzle cathode flows toward the workpiece and is directed downward, flowing on the sides of the cathode. This provides nonuniform current distribution at the part of the workpiece that is in contact with the electrolyte. The current, and hence the metal-removal rate, attains a high value in the impingement region, while a gradual drop in current as a function of the distance away from the impingement region leads to low metalremoval rates in these regions. Scanning the cathode or the sample serves to equalize the distribution of metalremoval rate by compensating for the stray-current effect, since every part of the sample undergoes both highcurrent and stray-current regions in cycle.

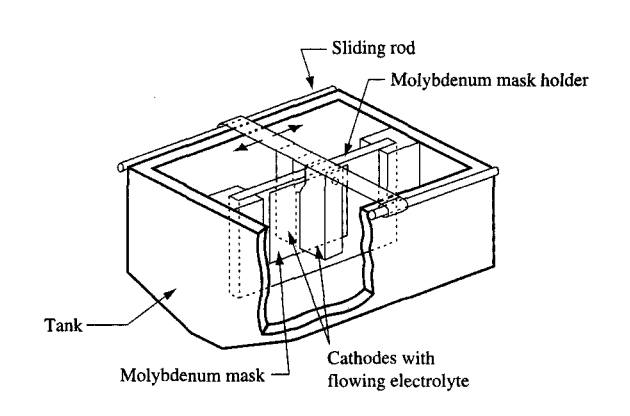
Figure 11 shows a two-sided EMM tool that was recently developed for high-speed fabrication of molybdenum masks [11]. The tool uses a novel concept of localized dissolution induced by scanning two cathode assemblies over a vertically held workpiece, providing movement of the electrolyte. Highly localized dissolution by using a small cathode width and an extremely small interelectrode spacing provide directionality of metal removal and uniformity of current distribution. The electrolyte flows through the cathode body at a rate between 0.8 and 3 gpm. It then flows across the cathode surface between the cathode and the mask anode. Two flow types were experimentally studied: shearing flow from top to bottom, and impinging flow directed into the mask anode. The cathodes were scanned back and forth across the vertically held anode mask at rates between 0.5 and 7 cm/s using an Anorad linear motion tool. Unlike many spray systems that are pressurized and involve solution spilling, the EMM tool is a nonpressurized system with electrolyte flowing in the downward direction. The tool is extremely flexible; it can handle different sample sizes and can employ different interelectrode spacings and electrolyte flow.

Fabrication of microelectronic components

As part of our continuing efforts to develop advanced metal-removal technologies, we have demonstrated the feasibility of EMM in the fabrication of a variety of microelectronic components. They involved the application of maskless and through-mask EMM in the fabrication of components such as print bands for high-speed printers [5], metal masks for screening and evaporation [15], inner planes for high-density circuitization [5], copper lines for printed-circuit boards [6], slider suspension for magnetic recording [19], cone connectors for pad-on-pad connector



Schematic diagram of an experimental tool for one-sided EMM (see Footnote 3).

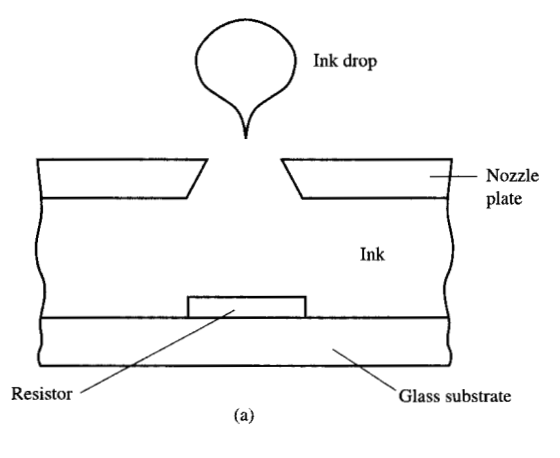


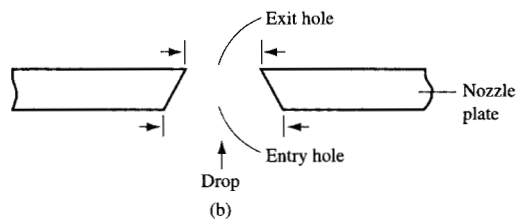
Schematic diagram of a prototype tool for two-sided EMM. From [15], reproduced with permission.

contacts [5, 25], and flip-chip interconnects [26]. In the following, some examples of the application of through-mask EMM are presented. The first three examples show the use of one-sided through-mask EMM to obtain patterns with precise angular walls, straight walls, and conical structures. The last two examples show the application of two-sided through-mask EMM in the fabrication of metal masks and in the drilling of patterns on thick metallic sheets for PC boards.

• Ink-jet nozzle plates

Ink-jet printing technology relies on the basic principle of forcing ink through a nozzle in the printer head. The driving force which causes the ink to be ejected from the





Schematic diagram of an ink-jet assembly showing (a) ejection of an ink drop through a nozzle plate, and (b) entry and exit holes of a nozzle plate. From [31], reproduced with permission.

nozzle is the formation of a high-pressure bubble, which is formed by rapid heating and vaporization of the ink constituents [Figure 12(a)]. The terms *entry hole* and *exit hole* in Figure 12(b) refer to the entry and exit of the ink drop during its ejection through the nozzle. Nozzles in the nozzle plate are evaluated in terms of their performance characteristics as measured by directionality, drop volume, drop velocity, and break-off uniformity. Printers that use arrays of nozzles are particularly sensitive to small differences in nozzle shape and dimensions. There are also constraints on materials and electrical and mechanical properties, as well as on the cost of the nozzle-plate material and fabrication process. Ink-jet printers used for computer output typically have nozzle diameters in the 40–100-μm range [27].

Different nozzle-fabrication techniques have been described in the literature [27–30]; they include mechanical drilling, etching of silicon and photosensitive polyimide, and electroforming. Mechanical drilling is expensive for low-end applications, since it frequently requires post-deburring treatment. Fabrication of precision nozzles has been demonstrated by anisotropic etching of silicon using silicon nitride as the mask, and by etching

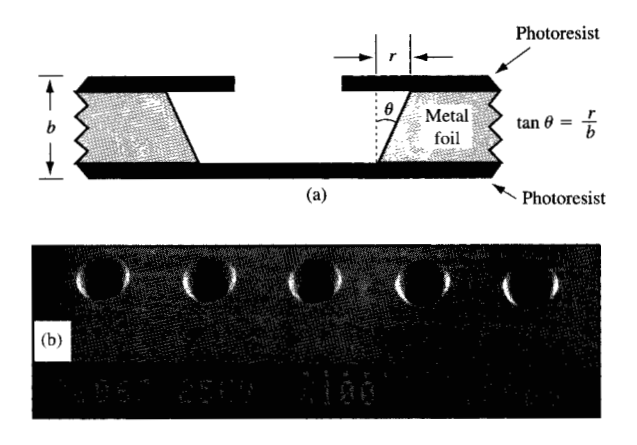


Figure 13

One-sided through-mask EMM with angular wall (a). SEM photographs of nozzles fabricated in 25- μ m-thick stainless steel foil (b). From [31], reproduced with permission.

of photosensitive polyimide [27, 29]. However, lack of mechanical strength and susceptibility to corrosion in the heated-ink environment have prevented the use of these materials on an industrial scale. Electroformed nozzles are currently used in ink-jet products manufactured by Siemens, Dataproducts, and Hewlett-Packard [27]. Electroformed nozzles are produced by plating nickel onto a mandrel (mold) which defines the image of the nozzle, and then removing the finished part [27, 28]. A thin protective film of gold is often used in cases where a particular ink otherwise might corrode the nickel. The electroforming process, however, is limited to materials that can be electroplated and is relatively expensive for low-end applications. In a recent publication we described a cost-effective, high-speed process for the fabrication of precision nozzles using through-mask EMM [31]. The process involves fabrication of a series of flat-bottomed, V-shaped nozzles in a metal foil. The process is applicable to a variety of materials including high-strength, corrosionresistant materials such as conducting ceramics. Throughmask EMM, therefore, provides the possibility of fabricating high-nozzle-density plates employing mechanically stable foil materials.

The fabrication of nozzle plates by EMM involves the following steps [31]. The cleaned metallic foil is laminated with photoresist on both sides of the foil. The photoresist on one side is then exposed and developed to define the initial pattern, consisting of an array of circular openings. A controlled EMM process is employed to fabricate flat-bottomed, V-shaped (frustum of right circular cone) nozzles on the sample. The photoresist is then stripped,

and the sample is inspected for entry and exit holes. A sample typically consisted of a series of photoresist-patterned nozzle plates, each containing thousands of exposed vias to be micromachined. A 25- μ m-thick stainless steel foil was laminated with 25- μ m-thick photoresist on both sides. The photoresist on one side was exposed and developed for patterning, while the blanket photoresist on the back side of the foil served as a protective insulating layer. The photoresist pattern consisted of an array of circular openings 55 μ m in diameter.

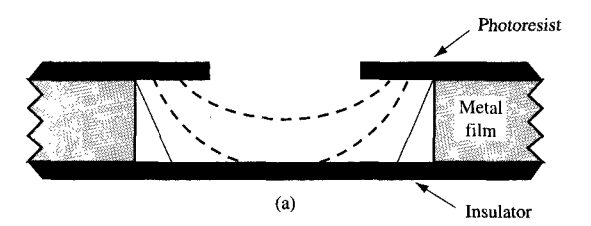
Direct- and pulsed-voltage experiments were performed using a neutral salt solution of sodium chloride and glycerol mixture as the electrolyte. The results demonstrated the importance of the role of masstransport-controlled limiting current and surface films in the fabrication of precision nozzles with smooth surfaces (Figure 13). By controlling the extent of micromachining, nozzles of desired shapes could be fabricated. The final nozzle shape was determined by several factors that included undercutting, etch factor, dissolution time, and dissolution conditions. Pulsating-voltage EMM was found to be effective in providing dimensional uniformity of an array of nozzles. This was due to the possibility of applying extremely high peak currents (voltage) which, in addition to giving directionality, enabled breakdown and elimination of inhibiting layers, thus facilitating activation of all of the openings at the same time. The feasibility of fabricating an array of hundreds to thousands of precision nozzles with microsmooth surfaces in copper and stainless steel foils was thus demonstrated. On a 25-\mu m-thick stainless foil patterned with a 55-µm-diameter photoresist opening, a targeted exit-hole dimension of 55 µm was achieved with a standard deviation below 2.0. A desired nozzle angle of 27° was produced with an etch factor (ratio of straight-through etch to undercut) of 2. The results of these studies conclusively demonstrated the effectiveness of through-mask EMM in the fabrication of precision nozzle plates for ink-jet printers [31].

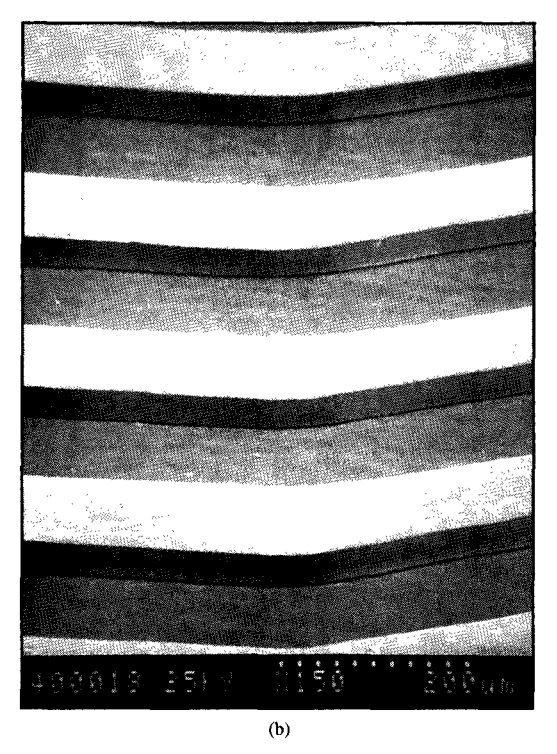
• Conducting lines for PC boards

Figure 14 shows the application of one-sided throughmask EMM in the fabrication of copper lines of varying dimensions for circuitization of printed-circuit boards [6]. This example of one-sided through-mask EMM involves fabrication of features with straight walls. A significant challenge in such an application is the ability to minimize undercutting to obtain finer and denser conductor lines.

• Cone connectors

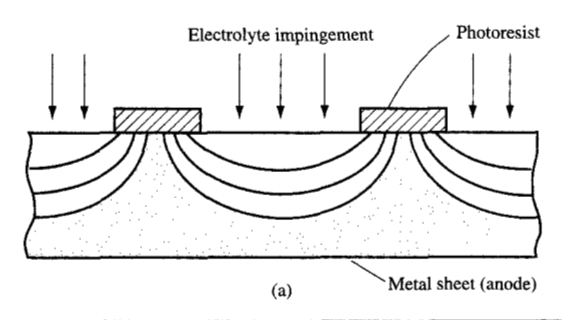
Cone connectors represent a new generation of connectors with low total load which find application in pad-on-pad cable connectors for flex, chip burn-in pads, high-





One-sided through-mask EMM of features with straight walls (a). SEM photograph showing bent copper lines with microsmooth surfaces and straight walls fabricated by one-sided through-mask EMM (b). From [6], reproduced with permission.

performance boards, etc. [32]. Effective cone-connector structures are characterized by small tips, tall cones, and strong material of fabrication. At present the cones are fabricated by laser ablation of polymeric films, followed by metallization. This technique produces relatively good-quality cones but involves several steps, thus making the process expensive. Furthermore, the cones fabricated by this method lack the desired mechanical strength. A high-speed process of fabricating cones by through-mask EMM has been developed and patented [25]. The process is applicable to a variety of metals and alloys and is independent of the hardness of the material.







One-sided through-mask EMM (a) and its application in the fabrication of cones with extremely fine (b) and flat (c) tips. From [25], reproduced with permission.

A photoresist pattern in the form of evenly spaced dots is generated on a metallic material that is suitably selected for the pad-on-pad connector. During EMM, the anode material dissolves in the areas which remain unprotected by the photoresist. As anodic dissolution continues, the removal of material between the dots leads to formation of cavities and finally to the formation of cones, as shown in Figure 15. Preferential dissolution in the desired direction is achieved by employing a multinozzle assembly in which extremely high impinging electrolyte flow can be applied. Cones on copper and hardened stainless steel (Fe-13Cr) sheets have been generated by this method. Figure 15 shows SEM microphotographs of the cones fabricated on a hardened stainless steel sheet. The desired size and shape of cones could be obtained by proper design of the photoresist dimensions and by properly controlling the amount of charge passed during EMM. By proper choice of electrolyte and machining conditions, many other metals and alloys can be used to fabricate such cones.

Metal masks

In the microelectronics industry, etched metal masks are used for pattern definition in conductor screening and

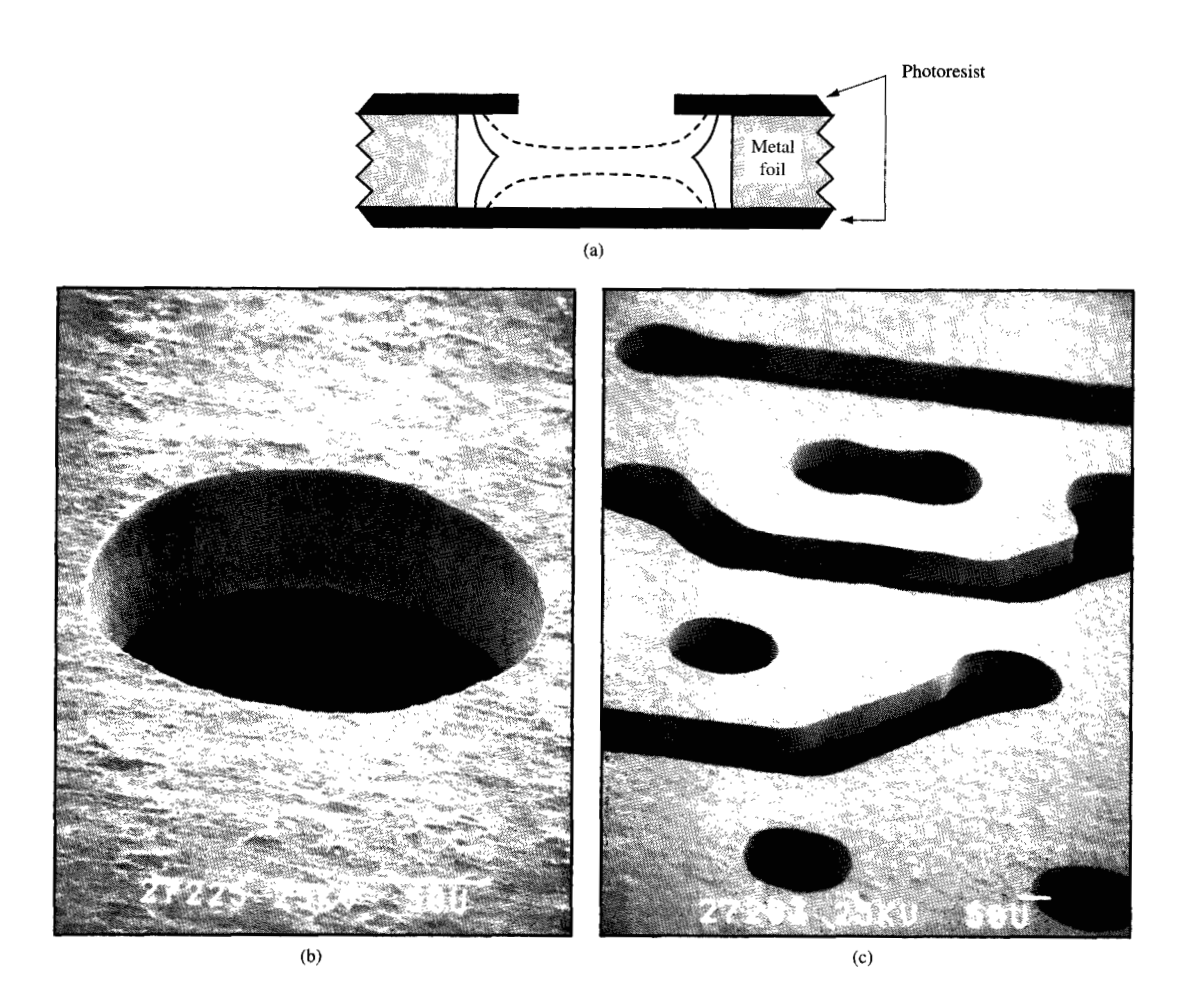
evaporation processes. Lead-frame production also requires patterned metal sheets that are either etched or stamped [33, 34]. Large volumes of patterned metal sheets are used in the production of aperture masks for color CRTs. A variety of metal and alloy sheets are used, including iron, stainless steel, copper, brass, and nickel–iron alloys. For the most demanding applications in screening and evaporation processes in microelectronics, molybdenum is the material of choice [32].

Fabrication of metal masks involves through-patterning by etching of a foil that is coated with perfectly aligned patterned photoresist on two sides. In a typical present-day processing, molybdenum masks are etched in a spray etcher using heated alkaline potassium ferricyanide solution. The solution will lose its etching activity as a larger quantity of the ferricyanide is reduced to ferrocyanide. Larger-volume users regenerate the etchant electrochemically or by using a chemical oxidizer such as ozone. The spent etchant must be disposed of as a hazardous waste. In addition, the rinse water from the etching operation must also be segregated and treated as a hazardous waste stream.

As an alternative, "greener" process, we have recently developed a novel EMM process for high-speed fabrication of molybdenum masks using a salt solution as the electrolyte [15]. A prototype precision tool of the type shown in Figure 11 was employed to fabricate molybdenum masks of different sizes (225 mm × 225 mm and 250 mm \times 250 mm). Features on the sheet, as many as 120000, were etched to a precision of 10% of the total feature size (Figure 16). The microfabrication data of EMM obtained in salt solution at ambient temperature were compared with those obtained by the conventional chemical etching process using ferricyanide solution. Performance criteria included machining rate, surface finish, aspect ratio, and simplicity of operation. The metal-removal rate in EMM was found to be orders of magnitude higher than that in chemical etching. Operating EMM at or higher than the limiting current density provided conditions for microsmooth surface and patterning uniformity. The ability to maintain a thin layer of soluble salt film at the surface was a key to obtaining uniformity of etching and high aspect ratio. Higher aspect ratio was achieved by increasing electrolyte impingement at the surface [15].

• Electrochemically drilled metal plates

In the manufacturing of printed-circuit cards and boards, it is often essential to drill holes in metallic plates [32]. Mechanical drilling of such holes poses several difficulties. Wear of drills, particularly for thick plates, is a major problem; drills must be changed frequently, thereby affecting cost and throughput. Chemical etching is an alternate technique which requires the use of aggressive



Two-sided through-mask EMM (a). Fabrication of molybdenum masks with vias and other complicated features (b), (c). Note that smooth surfaces and straight walls are obtained by EMM [15].

chemicals. The principal problems of chemical etching for such an application are its inability to yield straight walls and high aspect ratio.

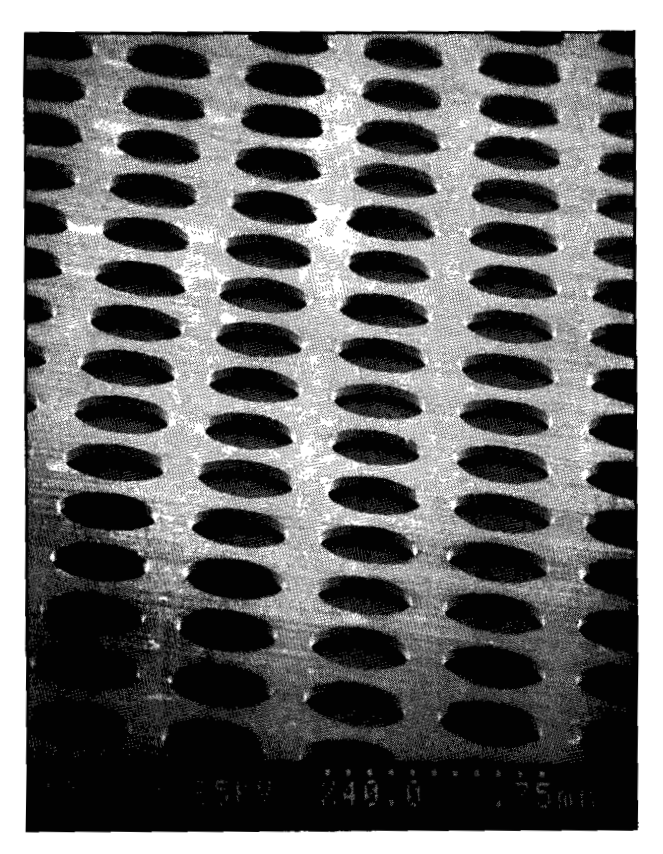
The electrochemical drilling described here involved two-sided through-mask EMM [5]. An example of electrochemically drilled holes in a 6-mil (125-\mu m)-thick stainless steel plate is shown in **Figure 17**. The electrolyte consisted of a 3-M sodium nitrate solution containing 100 ppm of FC-98 as a surfactant. The SEM photograph of Figure 17 shows that straight walls with extremely polished surface can be obtained. The operating cell voltage was determined from a study of the influence of cell voltage on the surface finish. In order to determine the conditions that lead to straight walls during electrochemical drilling, the influence of the quantity of charge on the shape

evolution was studied. Results indicated that knife-edgeshaped holes are obtained at low charges, while straight walls are obtained at high charges [5]. Similar electrochemical drilling studies have been extended to samples with extremely complicated shaped features of various dimensions.

Summary and conclusions

Metal-removal processes play an important role in the fabrication of microcomponents. Different dry and wet thin-film etching processes that are applicable in microfabrication are compared in **Table 1**, which provides information on the applicability of these processes. While dry-etching processes are particularly suitable for patterning fine dimensions, low etching rate and high equipment cost restrict their application to precision

⁴ M. Datta and W. J. Yu, unpublished work.



SEM photograph showing series of vias microdrilled by two-sided through-mask EMM in a 6-mil (125- μ m)-thick stainless steel sheet (see Footnote 4).

etching of thin films involving very small amounts of material removal. Wet chemical etching methods are used in microfabrication because of their selectivity and relatively high etch rates. These methods are predominantly used in large-scale production of metallic parts involving bulk metal removal. On the other hand, treatment and disposal of hazardous waste contribute

significantly to the product cost in many wet-etching manufacturing processes.

The last column of Table 1 presents some of the virtues of electrochemical metal removal as a thin-film processing technology. Since the driving force for metal dissolution reaction is derived from an external current, the electrolyte does not have to be aggressive. Neutral salt solutions are applicable for electrochemical micromachining of most of the thin metallic films that are of interest in the microelectronics industry. Metal removal in EMM is determined by the machining current, which can be very high if proper hydrodynamic conditions prevail within the electrochemical cell. Metal-removal rate in EMM is generally orders of magnitude higher than that in chemical etching. Through proper consideration of mass transport and current distribution, metal-removal rate in the lateral direction can be significantly influenced, thus providing better wall slope control in EMM. Other advantages include minimized safety and environmental concerns. All of these features make the EMM process a cost-effective, environmentally friendly processing technology for microfabrication.

While the application of electrochemical metal removal for metal shaping and finishing of large parts is not a new area, it is only now that the advantages of its application in microfabrication are receiving increasing recognition. Recent investigations of the development of the EMM process for microelectronic fabrication have been reviewed in this paper. Results of these studies indicate that the application of electrochemical metal removal in microfabrication offers many opportunities that have not hitherto been explored. Newly emerging technologies such as microengineered structures, advanced microelectronic packaging, sensors and microelectromechanical systems (MEMS) provide ample opportunities for further investigation of EMM. It is envisaged that with a better understanding of the principles involved in high-rate anodic dissolution of metals from narrow cavities, EMM will become an increasingly important processing technology for microfabrication.

Table 1 Comparison of dry and wet thin-film etching processes.

Etching factors	Dry etching		Wet etching	
	Ion etching	RIE	Chemical	Electrochemical
Driving force	Plasma	Reactive gases	Etching solution	External current
Environment	Vacuum	Vacuum	Acidic/alkaline solutions	Mostly neutral salt solution
Rate	~100 Å/min	\sim 1000 Å/min	$\sim 1 \ \mu \text{m/min}$	10 μm/min
Selectivity	Poor	High	High	High
Wall slope control	Directional	Anisotropic (flexible)	Isotropic	Better than chemical
Safety and environmental concerns	Low	Moderate/high	High	Low
Monitoring and control issues	Some	Some	Many	Few
Cost	High	High	Moderate	Low

References

- 1. J. L. Vossen and W. Kern, *Thin Film Processes*, Academic Press, Inc., New York, 1991.
- O. A. Moreno, R. C. McHatten, R. S. Paonessa, and R. H. Magnuson, in *Principles of Electronic Packaging*,
 D. P. Seraphim, R. C. Lasky, and C. Y. Li, Eds., McGraw-Hill Book Co., Inc., New York, 1989.
- J. A. McGeough, Advanced Methods of Machining, Chapman and Hall, New York, 1988.
- 4. W. J. McTegart, *The Electrolytic and Chemical Polishing of Metals*, Pergamon Press, London, 1956.
- M. Datta, "Electrochemical Micromachining," in Electrochemical Technology: Innovations and New Developments, N. Masuko, T. Osaka, and Y. Ito, Eds., Kodansha/Gordon and Breach, Tokyo, 1996.
- M. Datta, *Interface* (The Electrochemical Society) 4, No. 2, 32 (1995).
- M. Datta, L. T. Romankiw, D. R. Vigliotti, and R. J. von Gutfeld, J. Electrochem. Soc. 136, 2251 (1989).
- 8. C. van Osenbruggen and C. de Regt, *Philips Tech. Rev.* 42, 22 (1985).
- 9. M. Datta, IBM J. Res. Develop. 37, No. 2, 207 (1993).
- M. Datta and D. Landolt, J. Electrochem. Soc. 122, 1466 (1975).
- Ř. C. Alkire and H. Deligianni, J. Electrochem. Soc. 135, 1093 (1988).
- J. R. Selman and C. W. Tobias, Adv. Chem. Eng. 10, 211 (1978).
- R. C. Alkire, H. Deligianni, and J.-B. Ju, *J. Electrochem. Soc.* 137, 818 (1990).
- 14 D. Landolt, R. H. Muller, and Ch. W. Tobias, J. Electrochem. Soc. 116, 1384 (1968).
- 15. M. Datta and D. Harris, Electrochim. Acta 42, 3007 (1997).
- M. Datta and D. Landolt, *Electrochim. Acta* 25, 1255, 1263 (1980).
- E. Rosset, M. Datta, and D. Landolt, J. Appl. Electrochem. 20, 69 (1990).
- R. C. Alkire and P. B. Reiser, J. Electrochem. Soc. 131, 2797 (1984).
- M. Datta and L. T. Romankiw, in *Electrochemical Technology Applications in Electronics*, L. T. Romankiw, M. Datta, T. Osaka, and Y. Yamazaki, Eds., PV 93-20, The Electrochemical Society, 1993, p. 123; U.S. Patent 5,284,554, February 8, 1994.
- R. V. Shenoy and M. Datta, J. Electrochem. Soc. 143, 544 (1996).
- R. V. Shenoy, M. Datta, and L. T. Romankiw, J. Electrochem. Soc. 143, 2306 (1996).
- 22. D. T. Chin and C.-H. Tsang, J. Electrochem. Soc. 125, 1461 (1978).
- 23. D. T. Chin and K.-L. Hsueh, Electrochim. Acta 31, 561 (1986).
- R. C. Alkire and T.-J. Chen, J. Electrochem. Soc. 129, 2424 (1982).
- M. Datta, D. E. King, A. D. Knight, and C. J. Sambucetti, U.S. Patent 5,105,537, April 21, 1992.
- M. Datta, R. V. Shenoy, C. Jahnes, P. Andricacos, J. Horkans, J. Dukovic, L. T. Romankiw, J. Roeder, H. Deligianni, H. Nye, B. Agarwala, H. M. Tong, and P. Totta, J. Electrochem. Soc. 142, 3779 (1995).
- W. J. Lloyd and H. H. Taub, in *Output Hard Copy Devices*, R. C. Durbeck and S. Sherr, Eds., Academic Press, Inc., New York, 1988.
- 28. Hewlett-Packard J. 36, No. 5 (1985), entire issue.
- E. Bassous, L. Kuhn, A. Reisman, and H. H. Taub, U.S. Patent 4,007,464, February 8, 1977.
- 30. K. Brooks, P. R. Smith, and T. E. Morris, U.S. Patent 4,282,533, August 4, 1981.
- 31. M. Datta, J. Electrochem. Soc. 142, 3801 (1995).
- 32. R. R. Tummala and E. J. Rymaszewski, *Microelectronics Packaging Handbook*, Van Nostrand Reinhold, New York, 1989, p. 905.

- K. Abate, in *High Rate Metal Dissolution Processes*,
 M. Datta, B. R. McDougall, and J. M. Fenton, Eds.,
 PV 95-19, The Electrochemical Society, 1996, p. 157.
- 34. S. Hall, Circuits Assembly, p. 56 (August 1992).

Received November 2, 1996; accepted for publication December 8, 1997

Madhav Datta IBM Research Division, Thomas J. Watson Research Center, P.O. Box 218, Yorktown Heights, New York 10598 (mdatta@vnet.ibm.com). Dr. Datta manages the Flip Chip Interconnect Technologies Department in the Advanced Silicon Technology Laboratory of the Thomas J. Watson Research Center. He is also an Adjunct Professor of chemical engineering at the University of Connecticut at Storrs. He received his B.S. degree in chemical engineering from the H.B. Technological Institute, Kanpur, India, his M.S. degree in engineering from the University of California at Los Angeles, and his Ph.D. from the materials science department of the Swiss Federal Institute of Technology (SFIT), Lausanne, Switzerland. In 1985 Dr. Datta joined IBM, where he has been working on the application of electrochemical technology in microelectronic fabrication. He has received the IBM 8th patent plateau award and holds 20 issued patents and several Technical Disclosures. Dr. Datta is the author and coauthor of more than seventy scientific papers. He is an advisory board member of the Journal of Materials Processing Technology and is co-editor of a series, New Trends in Electrochemical Technology, published by Gordon & Breach. He is a divisional chair of the International Society of Electrochemistry (ISE) and treasurer of the electrodeposition division of the Electrochemical Society (ECS). He received the 1998 Electrodeposition Research Award of the Electrochemical Society. From 1995 to 1997, Dr. Datta was an active member of the National Electronics Manufacturing Initiative (NEMI), where he chaired the technology working group and the technology implementation group of energy storage systems.

[[Page 670 is blank]]